

The Greener Side of Polyoxometalate: As an Efficient Photocatalyst for Degradation of Phenol from Contaminated Water Source

¹Arabinda Mandal and ²Rajarshi Chatterjee*

^{1,2}Assistant Professor, Department of Chemistry, Bidhannagar College, Saltlake, Kolkata-64

Email: rajuchacha.2009@gmail.com

Abstract

The increasing amount of hazardous micro-pollutants in the aqueous environment has recently become a concern, especially because they are not usually included in environmental monitoring programs. Phenolic compounds, the most common toxic environmental pollutants, discharged as waste water from many industries are required to be removed. Usually phenolic wastes are treated by physicochemical methods like adsorption, reverse osmosis, electrolytic oxidation, and bioremediation. These methods are impractical due to high costs and the production of other toxic end products, e.g. conversion of phenol into chlorophenol when chlorination is used. Among various techniques available for removing phenol, biological treatment has been proved to be very effective. Again biological degradation usually takes longer time. Investigation of alternative economically viable pathways is the prime objective of our research work. Here we have examined the photocatalytic degradation of phenol from laboratory samples and petrochemical industries waste water under UV radiation by using nanoparticles of titanium dioxide embedded in polyoxometalates (POM). In this article, Lacunary Keggin heteropolyoxometalate $H_4[PVMo_{11}O_{40}]$ supported on TiO_2 nanoparticles was prepared by the solvothermal method. Characteristics of nano particles studded Keggin structure in the nano composites were confirmed by FT-IR and XRD analyses. The detailed information of POM-decorated nanoparticles is obtained by the combined use of scanning and transmission electron microscopy (SEM & TEM) along with thermo gravimetric analysis (TGA). The photocatalytic activity of prepared $H_4[PVMo_{11}O_{40}] / TiO_2$ for degradation of phenol under UV light was investigated using H_2O_2 as an oxidant. The results indicated that synthesized nano photocatalyst could be considered as an effective economic tool in the removal of organic pollutants from aqueous solutions in future.

Keywords

Photochemical degradation, Phenolic wastes, POM motivated nano particles

1. Introduction

The burning problem that can threaten the water ecology and public health is the toxic compounds that can get released in environment through industrial waste water [1]. Among the chemical wastes, the phenol and its derivatives are mainly prevalent in industrial effluent. Due to preferential stability in environment, high water solubility, high toxicity, and associated health problems, phenol removal from industrial waste water is very important [2]. Furthermore, phenol is known as a potential human carcinogen which raises considerable health concerns even at low concentrations. The United States Environmental Protection Agency (USEPA) has classified phenol as a priority pollutant [3]. So, it requires urgent removal of the waste stream before discharge to the environment. World Health Organization (WHO) recommended that phenol concentration in water resources entering conventional water treatment must be $<2 \mu\text{g/L}$. Furthermore, the concentration of phenol, chlorophenols, 2,4,6 trichlorophenol in drinking water must be $<0.1 \mu\text{g/L}$ [4]. Several technologies like adsorption, biological treatment, coagulation and flocculation, precipitation, distillation, solvent extraction, membrane process, and advanced oxidation have developed to remove phenol from water and waste water [5]. However, most of these techniques have some drawbacks including low efficiency, generation of secondary pollutants, high costs, etc. Bearing in mind the advantages of photochemical degradation, we worked on this process which could be an eco-friendly solution for the removal and degradation of micro pollutants in the aquatic environment to non-toxic final products such as CO_2 and H_2O . Photocatalytic degradation is an advanced oxidation process (AOP) that uses semiconductors and a light source to remove pollutants [6]. The advantages of AOP are in their low cost stability and high efficiency. Here we synthesized TiO_2 –POM nano particles and attempted to exhibit an application of AOP (UV/ TiO_2) for phenol removal from industrial and petrochemical wastewater. Polyoxometalates or POMs are so thoroughly discussed in several papers that they need no more detailed introduction. These are metal–oxygen cluster-anions, containing condensed metal-oxygen $\{\text{MO}_x\}$ polyhedral ($x = 4$ to 7), having metals (addenda atoms) like tungsten, molybdenum and vanadium in their higher oxidation state due to their appropriate ionic size and their ability to act as good acceptors of oxygen's electrons. The most commonly studied POM is the heteropolyacid (HPA) best represented by Keggin. [7] The arrangement of twelve metal atoms (e.g. $M = \text{V}, \text{Mo}, \text{W}$) around one single heteroatom (e.g. $X = \text{Si}, \text{P}, \text{As}$ etc.) forms a Keggin based POM, where $X/M=1/12$. In the Keggin structure, the heteroatom X is bonded to four oxygen atoms to form a tetrahedron and each metal atom is linked to six oxygen atoms to form octahedral. The assembly of three octahedra yields a trimetallic group M_3O_{13} which are connected to others and the common site of M_3O_{13} is linked to the central heteroatom X . In summary, there are four M_3O_{13} gathered around the central heteroatom X to form $(\text{XO}_4)\text{M}_{12}\text{O}_{36}$. In this paper, the synthesis of a mixed addenda Keggin type heteropolyacid (HPA) will be described and characterized. HPA typically has low surface area and high solubility, which makes it challenging to use them as catalytic materials in aqueous media. The cooperative chemistry of polyoxometalates (POMs) and metal nanoparticles (NPs) still remains a relatively unexplored area of nano science despite showing remarkable potential and application in fields as diverse as catalysis and medicine. Titanium dioxide (TiO_2) nanoparticles (NPs) are manufactured worldwide in large quantities for use in a wide range of applications. To make it more economically viable, different strategies are adopted. Keeping in mind the recent developments in the synthesis of nanoparticles using polyoxometalates

(POMs), we have tried to bring a new synthetic line for producing TiO_2 - nanoparticles. Many procedures can be foreseen to fabricate POM-based nanostructures, but solvothermal synthesis of nano oxides is a novel method till date. Not only this, numerous examples of POM-protected metal nanoparticles syntheses and reactions can now be found in the literature, [8] but the use of Keggin POMs to prepare nano-scale analogs of binary inorganic materials like metal-oxides is completely a new pathway which can be considered as the latest development. In short, solvothermal synthetic method of nano materials from gigantic POMs is undoubtedly a pioneer work when nano synthesis is concerned.

2. Experimental

Materials and methods

Chemicals were readily available from commercial sources and were used as received without further purification. The concentration of phenol was analyzed using the standard potassium ferricyanide method (EPA 420.1) [9]. Phosphovanado molybdic acid $\text{H}_4[\text{PVMo}_{11}\text{O}_{40}]$ (PVMA) was prepared according to the published procedure and characterized by IR spectroscopy [10]. Petrochemical wastewater was collected from Haldia refineries, located in West Bengal, India. Deionized water was used as the solvent.

Solvothermal synthesis of $\text{H}_4[\text{PVMo}_{11}\text{O}_{40}]$ stabilized TiO_2 nano particles (TiO_2 -PVMA)

The synthesis of POM modified nano TiO_2 was carried out as follows: 0.2 g of $\text{H}_4[\text{PVMo}_{11}\text{O}_{40}]$ (PVMA) was dissolved in 1 mL ultrapure water. 9 mL of concentrated HCl (37%, 12M) was added and charged to a 45 mL Teflon sleeve. 0.6 mL of titanium tetra isopropoxide $\text{Ti}[\text{OCH}(\text{Me})_2]_4$ (TTIP) was mixed with 19.4 mL of hexane and this mixture was carefully added into the Teflon without mixing with the aqueous layer. The Teflon was then sealed in a stainless-steel autoclave and heated at 170 °C for 24 h. The resulting TiO_2 was collected after cooling and washed 3 times with a mixture of 10 mL of water and ethanol (50% v/v) and dried in a vacuum oven at 40 °C for 24 h. This customized TiO_2 was dispersed into an absolute ethanol solution containing 3-Aminopropyl triethoxysilane (APTES) (1.5 % v/v) and magnetically stirred for 24 h for surface aminization. APTES is used here for covalent attaching of organic films to metal oxide titania TiO_2 . It is then centrifuged and washed with 10 mL ethanol 3 times before being dried in a freeze dryer for 24h. The surface-aminated TiO_2 was then dispersed into 15 mL absolute ethanol containing 0.2 g of $\text{H}_4[\text{PVMo}_{11}\text{O}_{40}]$ and stirred for 24 h. The resulting POM based TiO_2 was washed until the yellowish coloration of $\text{H}_4[\text{PVMo}_{11}\text{O}_{40}]$ was no longer observable and then freeze dried for 24 h before used for further application.

Physical measurements

Elemental analyses were carried out using a Perkin-Elmer 240 elemental analyzer. Spectral measurements were made in a Varian Cary 1E UV-visible spectrophotometer with 1.00 cm glass cells. IR (400–4000 cm^{-1}) was recorded in KBr pellets on a Nicolet Magna IR 750 series-II FTIR spectrophotometer. The morphology and elemental analysis of the as-synthesized TiO_2 and PVMA modified material was analyzed by a field

emission scanning electron microscope (FESEM JEOL-7600F). Powder XRD patterns were obtained by Bruker D8 advance diffractometer with monochromatic $\text{CuK}\alpha$ ($\lambda = 1.5418 \text{ \AA}$) with step size of $0.02^\circ \text{ s}^{-1}$. Thermo gravimetric analysis (TGA) was performed using TA instrument TGA Q500. Temperature was ramped up from room temperature to 100°C at a rate of $5^\circ \text{C min}^{-1}$, held isothermally at 100°C for 15 mins, ramped up to 200°C at a rate of $10^\circ \text{C min}^{-1}$. It is then finally and ramped up to 500°C at $10^\circ \text{C min}^{-1}$. Sample was dispersed in ethanol and dripped onto a copper grid with holey carbon support to study the local structure using a transmission electron microscope (TEM JEOL-2100F) at an accelerating voltage of 200 kV with a point to point resolution of 1.9 \AA .

3. Results and discussion

3.1. Vibrational and UV-vis- spectra

The synthesis of Keggin type phosphovanadomolybdic acid (PVMA) lays the foundation for the preparation and modification of materials. Using FTIR spectroscopy, the characteristic bonding in the PVMA were identified. The characteristic peaks of the Keggin structure can be found in the range of $1100 - 700 \text{ cm}^{-1}$. The main features are from P-O_a bonding of the centre tetrahedral, $\text{M-O}_b\text{-M}$ corner sharing bridging oxygen, $\text{M-O}_c\text{-M}$ edge sharing bridging oxygen and M=O_t terminal oxygen (where $\text{M} = \text{Mo}$ or V). The characteristic bands of P-O_a , M=O_d and $\text{M-O}_b\text{-M}$ in PVMA undergoes red shift with increase in vanadium substitution, which likely originates from the weaker metal oxygen bond due to vanadium (+5) being in a lower oxidation state than molybdenum (+6). Five strong vibration bands are indeed observed for, $\nu(\text{V=O})$, and $\nu(\text{V-O-V})$ at 1104.8 , 1060 , 957 , 889 , and 796.5 cm^{-1} . Apart from these, the IR spectrum of the title compound has some characteristic bands for the polyoxoanion at 510 , 940 , 878 , 770 and 1320 cm^{-1} which are attributed to $\nu(\text{V=O}_t \text{ terminal})$, $\nu(\text{V-O}_b\text{-V})$ octahedral edge sharing) and $\nu(\text{V-O}_c\text{-V})$ octahedral corner sharing) respectively. [9] In addition, a strong broad peak observed at 3350 cm^{-1} is assigned to $\nu(\text{-OH})$ absorption along with the hydrogen bonds which proves the presence of lattice water. Again, from the UV-visible spectral point of view, it has been observed that the formation of POM stabilized TiO_2 nano-composites resulted in a red-shift as shown in UV-vis diffuse reflectance spectra of TiO_2 , $\text{H}_4[\text{PVMo}_{11}\text{O}_{40}]$ (PVMA) and TiO_2 -PVMA composite. (Fig-1)

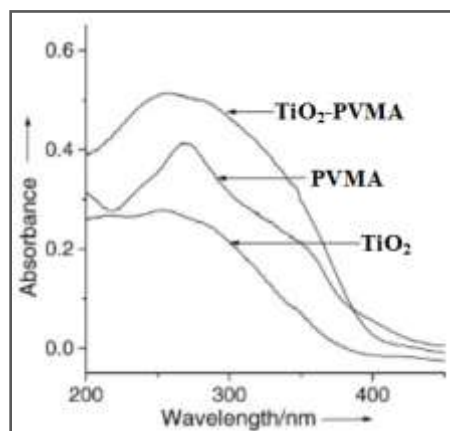


Fig-1: Comparative study of UV-vis spectra of TiO₂, PVMA and TiO₂-PVMA composite

3.2. Crystal structure

Polyoxometalates generally form ionic crystals [10] which can accommodate lattice water of crystallization and counteraction within the large interstices formed due to the size of the heteropolyanion and the requirement due to their huge ionic charge. The removal of water is easy and reversible by simple increment of temperature up to 150°C. Thus lattice water plays an important part in the crystal structure and packing of the heteropolyanion. Therefore, variation in the structure of polyoxometalate makes it difficult to obtain highly reproducible X-ray crystallographic information especially when powdered material is used instead of single crystal samples. That is why we prepared XRD sample mainly from single crystals. The powder XRD patterns of PVMA exhibits the diffraction peaks which show that the PVMA prepared consist of mainly a single crystalline phase. The lattice parameters of the crystals are close in values with H₄[PVMo₁₁O₄₀] having a =12.862Å and c =18.292 Å, with the incorporation of increasing number of vanadium atoms in place of molybdenum, the influence on the XRD peak position and intensity is minute. The small reflection peaks appearing in the diffraction patterns of PVMA are common, especially in powdered samples due to loss of water molecules which easily influence the crystal structure of PVMA. Our aim was to attain morphological control along with PVMA incorporation in the TiO₂ crystals. The combined XRD diffractogram given below (Fig-2) indicates that desired incorporation of PVMA in the TiO₂ crystal lattice via electrostatic interaction.

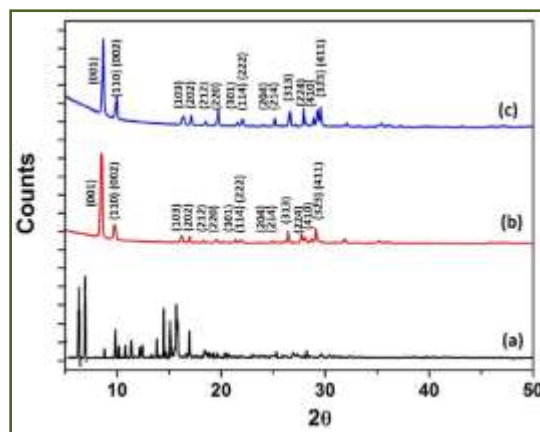


Fig-2: XRD diffractogram of (a) TiO₂, (b) PVMA and (c) TiO₂-PVMA with the characteristic reflection peaks of the Keggin structure labeled.

3.3. Thermo gravimetric analysis

Figure 2 shows the thermo gravimetric weight loss profile of PVMA. The crystal effloresces slowly even at room temperature and the large amount of water of crystallization which are loosely attached are easily lost as temperature increases. It can be seen that the sample experiences major weight loss as the temperature increases up to 100 °C. The temperature setting for the analysis was made to hold at 100°C and 200°C so as

to remove the water of crystallization completely. The 2nd derivative weight loss peak appearing around 300°C is associated with the removal of the structural water molecules holding the secondary structure of the PVMA. The calculation from the overall weight loss reveals that water of crystallization and chemical formula of the PVM prepared to be $H_4[PMo_{11}VO_{40}] \cdot 32H_2O$.

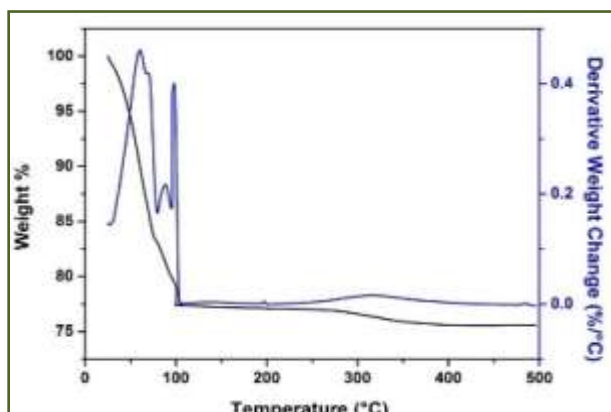


Fig-3: Thermo gravimetric analysis weight loss profile of complex 1

3.4. Characterization of TiO_2 -PVMA

With the aim of heterogenizing PVMA via immobilization, one-pot solvothermal synthesis was designed to incorporate $H_4[PVMo_{11}O_{40}]$ into the crystal lattice of TiO_2 . The desired outcome was to attain morphological control along with PVMA incorporation in the TiO_2 crystals for the final product which shows nano-plate morphology. In order to improve the coupling of PVMA with the TiO_2 surface, 3-Aminopropyl triethoxysilane APTES was employed as a coupling agent. The immobilization of PVMA on TiO_2 using a coupling agent increases the relevant elements of PVMA detected, but does not lead to formation of detectable PVMA crystalline phase. Nisar et al [12] showed that the main influence on post-modification was a decrease in the reflection intensity, which can be attributed to the reduction in reflected X-ray due to the surface modification. Further attempts to reduce the number of steps required in synthesis by introducing APTES in the organic phase during synthesis for surface modification proved to be futile and resulted in poor morphological control. This reveals that polyoxometalates are capable of stabilizing and protecting metal nanoparticles (NP) during their formation. [13] Figure 3(a) shows the SEM micrograph and (b) shows the TEM images of TiO_2 NP. Figure 3(b) also shows that the nano-plate is highly crystalline with clearly observable lattice.

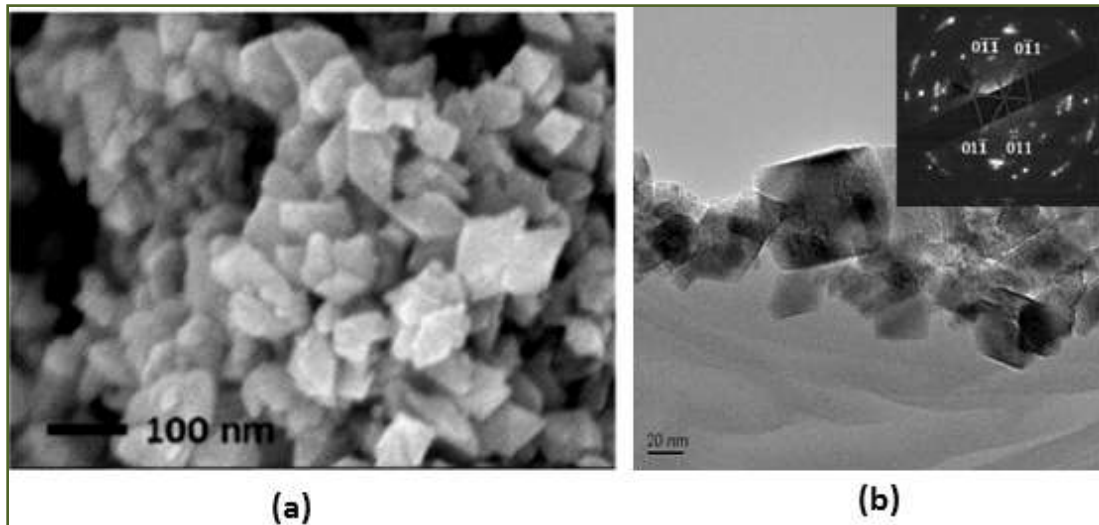


Fig-5: a) SEM micrograph of PVMA modified TiO₂ b) TEM micrograph of TiO₂ nanoparticles

4. Photo degradation of phenol

For photochemical degradation of phenol, a stock solution of phenol in water with a concentration of 1000 ppm was prepared. The working solution was prepared by diluting the stock solution with pH adjustment using 0.1(N) NaOH / HCl and transferred to Pyrex glass reactor of 100mL capacity. After preparing a working solution, an appropriate amount of TiO₂-PVMA catalyst was added to the phenol solution and it was stirred in dark conditions to ensure adsorption-desorption equilibrium. Then, the appropriate amount of H₂O₂ as an oxidant was added to the solution, and the system was irradiated with a 150W mercury lamp [14]. At the end of each experiment, one sample was taken from the system and was analyzed for determining phenol concentration after removal of nano- catalyst using centrifugation. An investigation program comprising five different phases were performed. Each phase corresponded to certain intensity of light and distance from UV source (15, 30, 50, 100, and 150 cm), initial phenol concentrations (30, 40, 60, 80, and 100mg/L), solution pH (3, 6.5, 9, and 11) contact time (from 0 to 300min), comparison of photocatalytic activities and phenol removal of Haldia Petrochemicals oil refinery waste water. All experiments were performed at 25°C.

4.1. Effect of intensity of light and distance from UV source

Distance of UV lamps from phenol solution and water was adjusted to 15, 30, 50, 100, and 150 cm. The results of the effects of intensity of UV source are shown in Fig-6. The phenol removal by photocatalysis was straight line decreased with the rising of UV lamps from reactor. As in Fig- 6, it appeared that optimum distance in which concentration reduction occurs most rapidly was 15 cm from surface of phenol solution. This may be due to lower light intensity and reduction of surface photocatalytic activities.

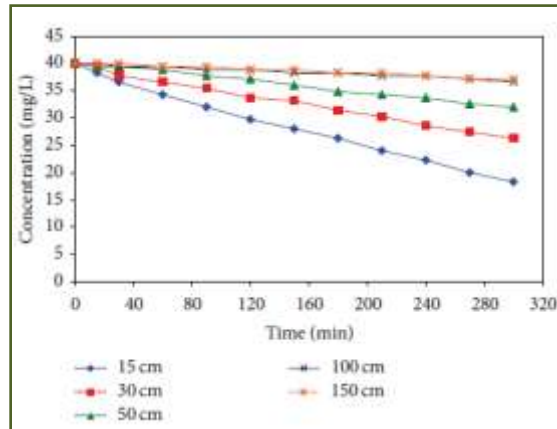


Fig-6: Effect of various intensities of UV lamps on (a) effluent phenol concentration

4.2. Effect of initial phenol concentration and phenol removal efficiency with contact time

To assess the effect of initial phenol concentrations, different concentrations of phenol, say 30, 40, 60, 80, and 100 mg/L were provided and were fed to reactor. Fig-7 showed the results related to of effect of initial phenol concentrations on photocatalysis phenol removal efficiency. From the graph it is clear that the phenol removal at initial concentration of 25, 30, and 40 mg/L by photocatalysis was about 50% at 300 min contact time. The percentage of phenol removal decreases with the mounting of the initial concentration of phenol from 50% to 20%. This could be due to the saturation of the surface coat of photocatalyst with by-product that resulted from degradation of phenol.

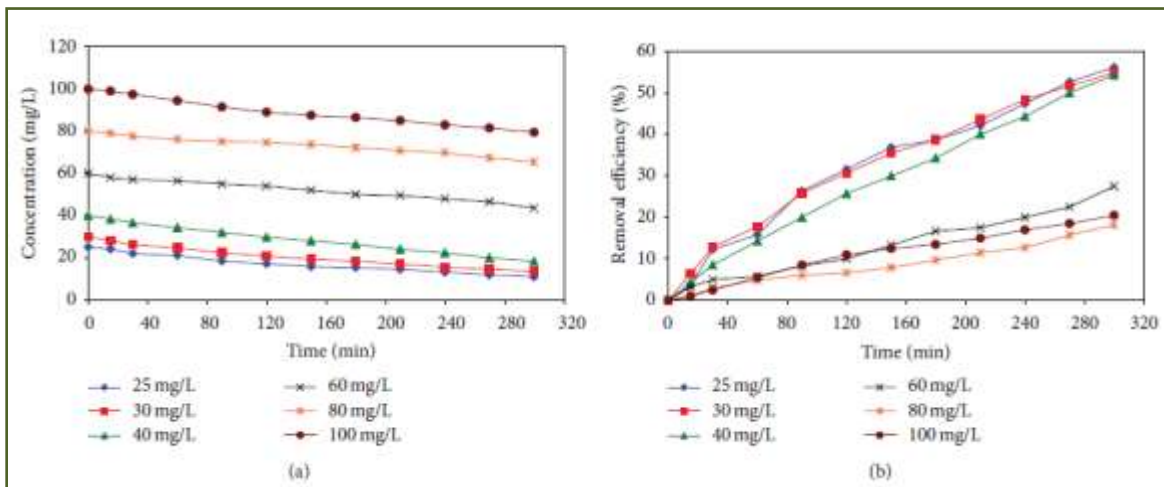


Fig- 7. Influence of initial phenol concentration and contact time (a) effluent phenol concentration and (b) phenol removal efficiency with contact time 0–300 min

4.3. Effect of pH

At different pH values, the reduction of phenol in aqueous solution was studied. Phenol solution with concentration of 45mg/L was provided; HCl and NaOH were used in order to adjust solution pH at values of 3, 6.5, 9, and 11. The results obtained are shown in Fig-8 which shows the effect of solution pH on the phenol removal from the aqueous solution by photocatalysis process expressed in terms of the effluent phenol concentration and phenol removal percentage. It is clear that phenol was effectively removed at solution pH 3. We have found that at this particular pH, phenol and allied phenolic compounds undergo complete oxidation to give safer compounds CO₂ and H₂O [15]. The reaction is as follows: C₆H₅OH + 7O₂ → 6CO₂↑ + 3H₂O.

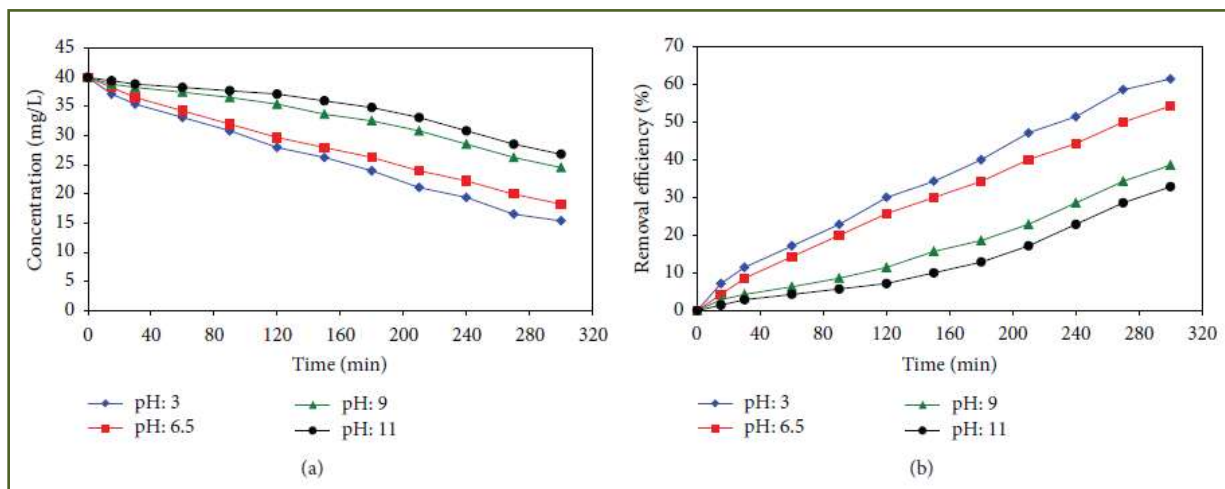


Fig- 8. Effect of solution pH on (a) effluent phenol concentration and (b) phenol reduction (C₀: 40mg/L, distance of UV source: 15, contact time 0–300 min, and solutions of various pH).

4.4. Comparison of photocatalytic activity

In order to compare photolytic activity, three parallel experiments are performed. Individual rate of degradation of phenol was observed for i) TiO₂ ii) PVMA iii) TiO₂-PVMA. It can be seen from Fig.9 that degradation of phenol was occurred at a high rate for all catalysts up to the first 20min of the process. After that, degradation of phenol continued at a lower rate. The degradation efficiency was almost reached equilibrium for TiO₂ and TiO₂-PVMA catalysts after 80min. However, PVMA as a homogeneous catalyst showed a relatively high rate of degradation until the end of the process, but the heterogeneous catalyst, TiO₂-PVMA showed the highest degradation efficiency and its efficiency reached to 90% at a contact time of 80min.

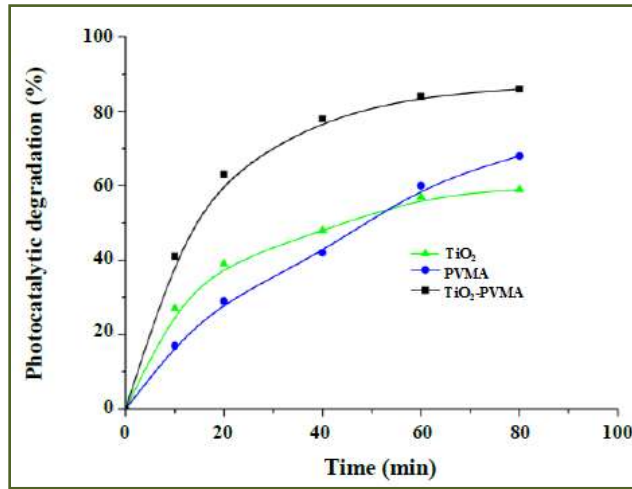


Fig-9. Photocatalytic activity of catalysts towards phenol

4.5. Phenol removal from Haldia oil refinery wastewater

The composition of the Haldia Petrochemicals oil refinery waste water varied as follows: phenol concentration (45mg/L) and pH (5.5). Fig-10 shows the evolution of phenol. The assessment of initial phenol concentration with respect to contact time and solution pH clearly revealed that that for lower concentration of phenol in wastewater, removal efficiency is higher. in this process, removal efficiency was higher in low solution pH. So with raising the solution pH from 3 to 11, phenol removal efficiency varied from 60% to 30%.

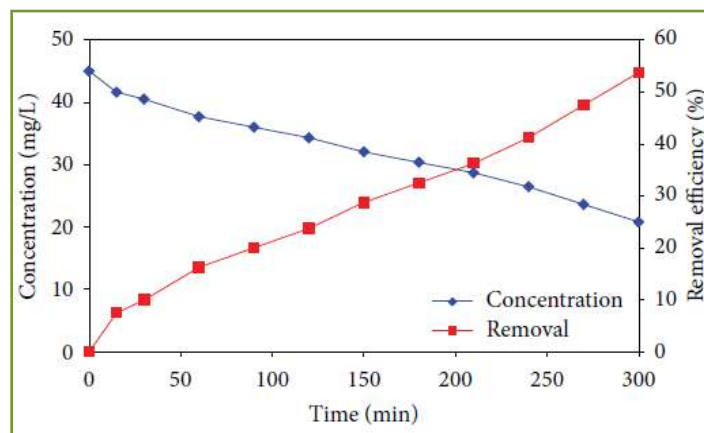


Fig-10. Phenol removal from Haldia oil refinery waste water with phenol concentration of 45mg/L

5. Conclusion

A nano photocatalyst of Lacunary Keggin-type hetero polyoxometalate studded with TiO₂ was successfully synthesized. Photocatalytic degradation of phenol with TiO₂-PVMA as catalyst and UV radiation is the

latest process till date. In this research, photocatalytic degradation of phenol with emphasis on contact time, solution pH variations, UV radiation and initial phenol concentration was assessed. These results indicated that increasing contact time and reducing initial phenol concentration led to improvement in the removal percentage of phenol. Results obtained from comparison of phenol degradation from laboratory sample and industrial wastewater showed that at similar conditions, the phenol removal was equal. Photocatalysis laboratory scale studies showed that this process could be suggested as an applicable method for removing phenol as toxic and dangerous matter from effluent and waste water by degradation and converting it into safe matter. These methods with advantages of production of non-hazardous by-products with high efficiency in comparison to the biological methods have potential to be a suitable purification mechanism in waste water industries in near future.

References

1. Eckenfelder W.W., Englande A. J. (1998) *Water Science and Technology*. 38: 111–120
2. Sawyer C., Carty P.(2003) *Chemistry For Environmental Science*, McGraw-Hill, New York.
3. Sullivan B.G., Krieger G.R. (2001). *Clinical Environmental Health and Toxic Exposure*.
4. Chang L., Chen, I-P., Lin S.S. (2005) *Chemosphere*. 58: 485–492
5. Zazouli M.A., Taghavi M., (2012) *J. Water Resource Prot.* 4: 980-983
6. Miklos D.B., Remy C. (2018) *Water Research*. 139: 118-131
7. Keggins J. F. (1934) *Proceedings of the Royal Society of London. Series A* 144: 75-100
8. Nisar A., Lu Y., Wang X. (2010): *Chemistry of Materials* 22: 3511-3518
9. APHA (2005) *Standard Methods for Examination of Water*. Washington, DC, USA.
10. Chatterjee R. (2018) *J. Emerging Techno and Innovative Research JETIR* 5: Issue 7: 98-104
11. Spirlet M., Busing W. (1978): *Acta Crystallographica B Structural Science* 34: 907-910
12. Nisar A., Lu Y., Wang X. (2010): *Chemistry of Materials* 22: 3511-3518
13. Wang Y., Weinstock I. (2013): *Nanoscience and Nanotechnology* 8: 1-47
14. Nasiryan M., Tabatabaee M. (2021): *Iran. J. Chem. Chem. Eng.* 40(5): 1414-1420
15. Jhonston P.K., Doyle E. (1988): *Journal of American College of toxicology* 7(2): 201-220